Indian Journal of Engineering & Materials Sciences
Vol. 32, February 2025, pp. 81-103
DOI: 10.56042/ijems.v32i01.12220

Effect of metakaolin and silica fume with polypropylene fiber on the properties of concrete pavement incorporating taguchi analysis

Ravi Kumar Meena[a*], Rameshwar J. Vishwakarma[a] & Jeetendra Singh Khichad[b]

[a]Department of Civil Engineering, Malaviya National Institute of Technology, Jaipur, Rajasthan 302 017, India
[b]Department of Civil Engineering, North Eastern Regional Institute of Science and Technology, Itanagar, Arunachal Pradesh 791 109, India

Received: 12 July 2024; accepted: 16 December 2024

This study has investigated the comparative effects of metakaolin (MK) and silica fume (SF), combined with varying dosages of polypropylene fiber (PPF), on the mechanical properties of M25 grade concrete used in pavement. SF and MK have been used to replace 10% of cement by weight, while PPF has been added in proportions ranging from 0.25% to 1%. The results have shown a decrease in workability with the addition of SF, MK, and increasing PPF content. Maximum compressive strength has been achieved with 10% MK and SF replacement, although PPF has had minimal impact on this property. Flexural and splitting tensile strengths have peaked at 0.50% and 0.75% PPF, respectively, while density has been lowest at 1% PPF. Taguchi and regression analyses have identified PPF as the dominant factor influencing flexural and tensile strength, while MK & SFhave primarily affected compressive strength. The combination of 10% SF or MK with 0.50% PPF has yielded the best performance in flexural strength, making it suitable for urban and rural concrete road pavements.

Keywords: Concrete, Mechanical properties, Metakaolin, Polypropylene fiber, Silica fume, Taguchi analysis

1 Introduction

In developing nations like India, the construction of roads is happening more quickly than in the past, and huge funds are allocated for road construction[1]. In India, there are two types of pavement materials: concrete and bituminous. Both pavement materials have their advantages and disadvantages. However, Concrete pavements appear more suitable for Indian conditions when considering factors like life-cycle cost, availability of local materials, and durability in adverse conditions like monsoon and unexpected traffic. The main challenge for concrete roads is their initial expense. In addition to reducing carbon emissions, using environmentally friendly materials is a significant step toward a sustainable future. Concrete roads are sustainable alternatives to lessen the negative environmental impact and improve the quality of the road network, as demonstrated by the various initiatives and their potential benefits[2–4].

Globally, concrete is the most commonly used material for constructing roads[5]. Increased cement demand increases fuel use, energy inputs, lime excavation, resource waste, and atmospheric CO_2 emissions. India is in 3rd place in the world in terms of CO_2 emissions, with a population of 1.4 billion. In the Paris Agreement 2015, India aims to decrease its carbon emissions per GDP unit by 33–35% by 2030 compared with 2005. 1 ton of cement releases a compelling amount of CO_2, producing up to 7% of the world's CO_2 emissions[6–8]. Furthermore, compared to alternative materials, the energy and emissions of greenhouse gases needed to process Portland cement are incredibly high[9]. The cement utilization cannot be avoided until the unanticipated future, and when constructing roads, it becomes more critical to partially replace supplemental cementitious materials (SCMs) with Portland cement[10]. It is the responsibility of the construction industry to take control of cement consumption by finding new ways. i.e., Granulated Blast Furnace Slag (GBFS), Silica fume (SF), Fly Ash (FA), Metakaolin (MK), and Rice Husk Ash (RHA) can reduce the cost of producing concrete and have positive effects on the environment[11–13]. SCMs are by-products of industries like thermal power plants, steel manufacturing, ceramics, ferrosilicon alloys, silicon metal, and copper manufacturing industries. SCMs are by-products; they do not require energy consumption and are sustainable materials in the construction industry. These SCMs impart strength and durability to concrete by acting as a filling agent. SCMs are pozzolanic materials with finely ground

*Corresponding author (E-mail: 2023rce9005@mnit.ac.in)

particles that enhance concrete mixtures' fresh and hardened qualities by replacing the OPC portion or whole[14].

The use of calcined clays as supplementary cementitious materials (SCMs) has attracted considerable attention in recent years[12,13]. Metakaolin (MK) is the most extensively studied and widely utilized[15–18]. MK can partially replace Portland cement in concrete mixtures. Producing one tonne of Portland cement typically requires 1.6 tonnes of clay and limestone, whereas manufacturing one tonne of MK requires approximately 1.16 tonnes of kaolin. While MK remains stable under normal climatic conditions, it undergoes a mass loss of about 14% during calcination at temperatures between 650°C and 900°C[17, 19]. The partial substitution of cement with MK improves various concrete properties, including flexural and compressive strength, resistance to chemical attack, and overall durability[20].

When SF is used in concrete, it is a very large reactive pozzolana due to its microscopic particles, larger surface area, and high silicon oxide content. SF quality is specified by AASHTO M 307 and ASTM C 1240[21]. SF is available in wet or dry forms for use in concrete. The SF content in concrete varies from 5% to 10%, depending on the desired end-use and the amount of superplasticizer. SF enhances concrete's bond strength, compressive strength, and abrasion resistance properties. SF reduces permeability and protects reinforcing steel from corrosion[22].

The concrete is poor in tension but good in compression. Concrete has high brittleness, less ductility, less impact toughness, and low tensile strength; due to these engineering properties, it has many limitations[23–27]. Arranging fibers randomly in concrete is among the best methods to enhance tensile strength, energy absorption capacity, energy captivation capacity, compressive strength, and the poor properties mentioned above[28]. An additional adverse effect observed is the formation of cracks in concrete samples due to inadequate dimensional stability. However, the incorporation of fibers in the concrete mix has been shown to reduce crack formation[29–31]. These reinforcing fibers are steel fibers[32], polypropylene fiber[33], glass fiber[34], basalt fiber[35], composite fiber[36–38], and natural organic fiber[39]. Polypropylenefiber (PPF) is a synthetic fiber. It is white in colour and made from PP polymerization. It has several advantages, such as being lightweight, highly tough, and corrosion-resistant[40]. According to the size, PPF is classified as micro and macro PPF[41]. While there are various benefits to using PPF with concrete, little research has been done to fully understand the nature of PPF's modification mechanism. This is especially the case when examining PPF's modification mechanism with the crystal structures and the aggregate-cement ITZ of PPF-reinforced concrete[42]. The various researchers previously investigated the utilization of waste in concrete production, introducing novel construction materials, procedures, design tools, and techniques to provide cost-effective, sustainable, and precise solutions to pavement construction[43, 44].

This study is consistent with several important Sustainable Development Goals (SDGs) as per the United Nations Development Programme (UNDP) Agenda 2030, which seeks to solve global challenges and attain an improved and more sustainable future[45]. The best five SDGs are easily associated with the research aims and findings from the study on the application of supplemental cementitious materials (MK and SF) and PPF in concrete pavements, as mentioned in Fig. 1. It improves the durability and resilience of concrete pavements (SDG 9), ensures safer and more reliable transport systems (SDG 11), promotes the efficient use of natural resources by reducing dependence on Portland cement (SDG 12), contributes to climate change mitigation by

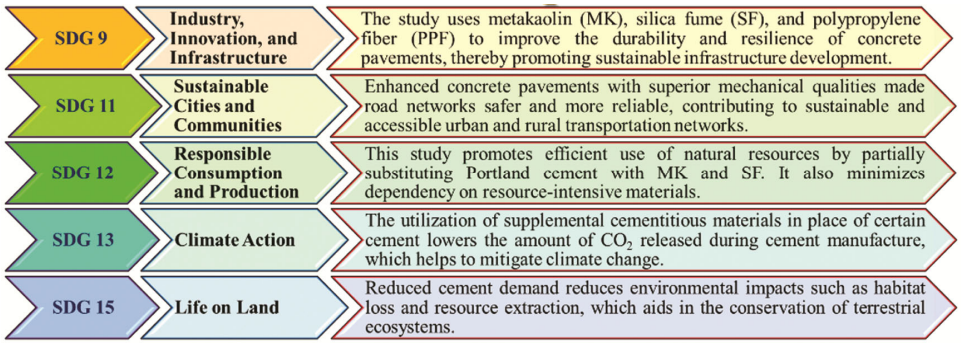

Fig. 1 — Alignment of this experimental study with the five key Sustainable Development Goals per UNDP.

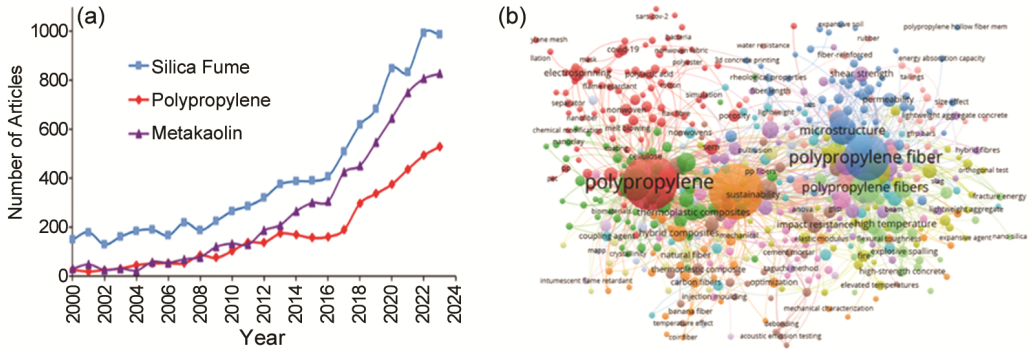

Fig. 2 — (a) Scopus year-wise published articles and (b) Co-occurrence from Scopus search.

decreasing CO_2 emissions (SDG 13), and promotes environmental conservation by reducing habitat loss and resource extraction (SDG 15).

1.1 Bibliographic analysis

The Scopus year-wise published articles in Fig. 2(a) show a significant increase in SF, MK, and PPF use since theyear 2000. The data indicates a dynamic and rising trend in material consumption, indicative of the period's technical developments and global economic recovery. The increase in demand for SF and MK is due to improved concrete properties, reduced environmental impact, reduced carbon footprint, and strength enhancement[16]. PPF demand increases due to enhanced concrete performance, crack control, improved impact resistance, and flexibility in design[42].

The data analysis on the published literature that was obtained from SCOPUS is covered in this part. The keyword searches "silica fume," "metakaolin," and "polypropylene" were used to find the data. Fig. 2(b) shows the term co-occurrence map with overlay visualization. According to Fig. 2(b), research on the functional gradation of concrete is currently popular, meaning that more studies in this field can be carried out, and the relationship between the keywords, which illustrates the range of studies done about the functional gradation of concrete. The map illustrates how the world is leading the way regarding its contributions to functional grading research in concrete.

1.2 Objective of the study

The main objective of this experimental study is to assess the concretes` workability and mechanical characteristics (flexural strength, split tensile strength, and compressive strength) using supplementary cementitious materials (SCMs). In this study, MK and SF each replace 10 % weight of the cement, and PPF is added in varying proportions up to 1 % of the cement content, at 0.25 % intervals.

Table 1 — Chemical composition of cement, MK, and SF.

Composition (%)	Cement	MK
CaO	64.7	51.3
SiO_2	21.6	0.2
Fe_2O_3	2.2	1.5
Al_2O_3	6.1	43.8
MgO	0.8	0.3
K_2O	0.6	0.4
Na_2O	0.1	0.1
SO_3	1.92	0.05

2 Materials & Methods

2.1 Materials

Ordinary Portland cement (OPC) of 43-grade cement locally available in the market is used in this investigation, adhering to various specifications of IS 8112: 2013[46]. OPC's specific gravity was 3.15, surface area 3000 cm^2/gm, bulk density 1450 Kg/m^3, and consistency was 33% as per IS 8112: 2013[46,47].

Table 1 provides information about OPC's chemical composition[46,47]. The fine aggregate consisted of river sand sourced from Banas Tonk, Rajasthan. The sand used passed through a 4.75 mm IS sieve and conformed to the specifications of IS 383:1970[48]. FA`s fineness modulus and specific gravity were observed at 2.727 and 2.65, respectively. This fine aggregate confirms Zone–II gradation according to IS: 383-1970[48]. For this experiment, coarse aggregate (CA) from nearby quarry units has been utilized. The maximum size used in this investigation is 20 mm and 10mm for CA. The specific gravity and the maximum water absorption were observed at 2.64 and 3.40%, respectively, from testing. Table 1 provides information about MK's chemical composition[47,49].The particle surface area and specific gravity were 700 m^2/Kg and 2.60, respectively. MK was prepared by calcinating kaolin at 800 °C for 4 hours, and MK's mineralogical and chemical composition[50]. MKs` Energy Dispersive

X-ray analysis (EDAX) and Scanning Electron Microscopy (SEM) images are shown in Fig. 3 (a,b)[49]. The X-ray diffraction (XRD) image of MK is shown in Fig. 3 (c)[51]. The EDAX analysis of MK indicates a high intensity of alumina and silica. This contributes to enhanced durability of the concrete, primarily due to the increased formation of secondary Calcium-Silicate-Hydrate (C-S-H) gel resulting from MK's high silica and alumina content[52]. X-ray diffraction (XRD) was employed to characterize the phase composition of the geopolymer composites[51]. MK-based geo-polymers produced two clear diffraction patterns corresponding to crystalline materials imprinted in the material (quartz, anatase, muscovite, etc.) by XRD analysis. The peak of unstructured material was found at 2θ of 27°–30°. which was approximately 5°-8° higher compared to the metakaolin peak at only 2θ of 22° in Fig. 3(c).

Table 1 shows the chemical properties of SF[49],while Table 2 shows the physical properties. Fig. 4 (a,b) shows the SF's SEM image and XRD graph, respectively[53].

The absence of apparent peaks in SF can be explained by its amorphous nature in Fig. 4. According to the XRD graph (Fig. 4b), the SiO_2 content has maximum intensity. The XRD study revealed that the age of the concrete and the concentration of SF affect the calcium hydroxide (CH) ratio created during hydration. As per SEM examination, the application of SF reduces gaps and C-S-H, which is also a hydration product.The non-absorbent PPF has a melting point of 165 °C, three distinct lengths of 6.0 mm, 12.0 mm, and 19.0 mm, and an equivalent diameter of 48 µm. The primary purpose of a superplasticizer is to enhance workability[54].

Enfiiq Super Plast 400 is the admixture with a high water-reducing range that was used in the experiments. According to the seller, the specific gravity of the superplasticizer at 30 ° C ranged from 1.175 to 1.190. The applied super-plasticizer dosage is 0.65% by weight of the cement. Fig. 5 displays the materials utilised in this investigation.

Table 2 — SF physical properties[54].

Properties	Values
Particle size (typical)	< 1 µ m
Bulk Density (as produced)	130 – 430 kg/m3
Bulk Density (Slurry)	1320 – 1440 kg/m3
Bulk Density (Densified)	480 – 720 kg/m3
Specific gravity	2.22
Surface area (BET)	13,000 – 30,000 m^2/kg

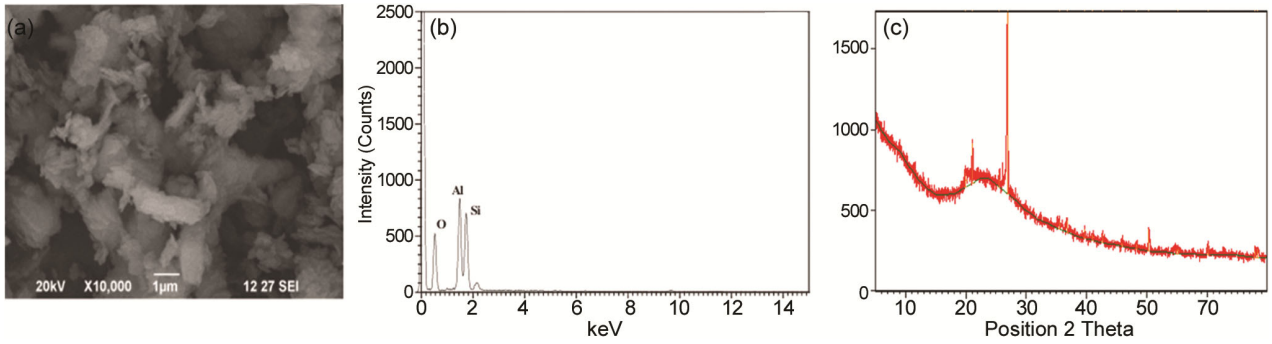

Fig. 3 — MK (a) SEM image[49] (b) EDAX graph[49] and (c) XRD graph.

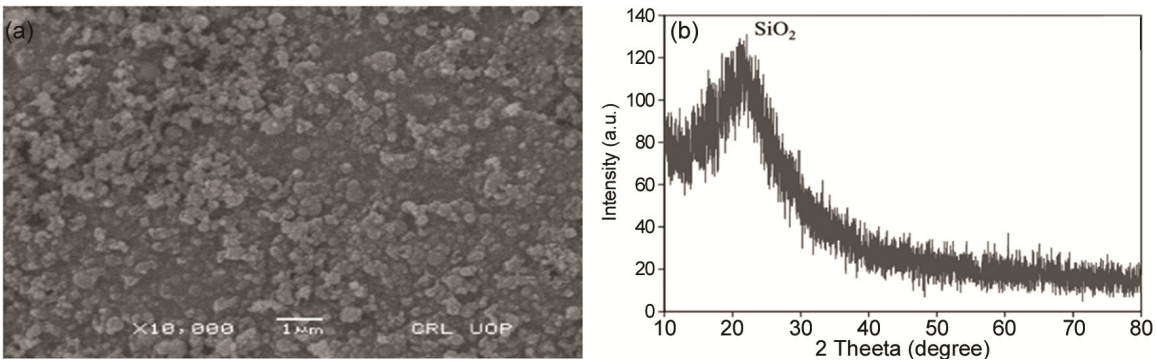

Fig. 4 — SF (a) SEM image[53] and (b) XRD graph[53].

Fig. 5 — Materials (a) Cement (OPC 43 grade), (b) Fine aggregates (FA), (c) Coarse aggregates (CA), (d) Polypropylene fiber (PPF), (e) Metakaolin (MK), (f) Silica fume (SF), and (g) Experimental materials.

Table 3 — Description of various concrete mixture samples.

Designated Name	Cement (%)	Metakaolin (MK) (%)	Silica Fume (SF) (%)	PPF (%)	CA (%)	FA (%)
CM	100	0	0	0	100	100
OMP0	90	10	0	0	100	100
OMP0.25	90	10	0	0.25	100	100
OMP0.50	90	10	0	0.50	100	100
OMP0.75	90	10	0	0.75	100	100
OMP1	90	10	0	1.00	100	100
OSP0	90	0	10	0	100	100
OSP0.25	90	0	10	0.25	100	100
OSP0.50	90	0	10	0.50	100	100
OSP0.75	90	0	10	0.75	100	100
OSP1	90	0	10	1.00	100	100

2.2 Mix design & testing methods

2.2.1 Mix proportion

IS 10262:2019 was followed in the concrete mix design to obtain the characteristic compressive strength of 25 N/mm^2.This grade (M25) is considered for performing the study of partial replacement of MK and SF in concrete.

In this comparative study, two concrete set mixes were prepared. In one set of concrete mixtures, 10% of the cement is replaced by MK; in another, 10% is replaced by SF. Each mix set contains five samples with percentage variations of PPF, i.e., 0%, 0.25%, 0.50%, 0.75%, and 1.00%, with a w/c ratio of 0.45. The mixture identity is assigned to a distinct mixture following the corresponding fractional replacement, shown in Table 3. According to IS 10262:2009, the calculated proportions of the mix design are mentioned in Table 4.

2.2.2 Workability

A slump test was conducted to ensure consistency across batches as a quality control measure for PPF, SF, and MK in fresh concrete mix. Their uniform distribution within the concrete influences the quality of the fibers, interaction with the cement matrix, and the ease with which the concrete can be sprayed or cast. The workability tests were conducted using a slump mould in standard sizes per IS: 7320 (1974)[55].

2.2.3 Compressive strength

Compressive strength is the main characteristic of hard concrete and is frequently used as a characteristic property for concrete classification[56]. 150 x 150 x 150 mm steel moulds were tested in a 2000-KN capacity compression testing machine after being permitted to cure for 7 and 28 days in a curing tank at standard temperature. The test procedures used per IS 516 (Part-1 Sec-I) – 2021[57]

Table 4 — Mix proportion forconcrete mix.

Mixture ID	Cement (Kg/m^3)	Metakaolin (MK) (Kg/m^3)	Silica Fume (SF) (Kg/m^3)	PPF (Kg/m^3)	CA (Kg/m^3)	FA (Kg/m^3)	Water (Kg/m^3)
CM	369.67	0	0	0	1046.71	826	166.35
OMP0	332.70	36.97	0	0	1046.71	826	149.71
OMP0.25	332.70	36.97	0	0.92	1046.71	826	149.71
OMP0.50	332.70	36.97	0	1.84	1046.71	826	149.71
OMP0.75	332.70	36.97	0	2.76	1046.71	826	149.71
OMP1	332.70	36.97	0	3.68	1046.71	826	149.71
OSP0	332.70	0	36.97	0	1046.71	826	149.71
OSP0.25	332.70	0	36.97	0.92	1046.71	826	149.71
OSP0.50	332.70	0	36.97	1.84	1046.71	826	149.71
OSP0.75	332.70	0	36.97	2.76	1046.71	826	149.71
OSP1	332.70	0	36.97	3.68	1046.71	826	149.71

2.2.4 Flexural strength

The steel moulds of 500 x 100 x 100 mm size were tested in a flexural testing machine after being permitted to cure for 28 days in a curing tank at standard temperature. The test procedures used as per IS 516 (Part-1 Sec-I) – 2021[57].

2.2.5 Split tensile strength

Concrete`s split tensile strength agrees with its flexural and compression performance[58]. The specimen shall be a cylinder, 300 mm long and 150mm in diameter, and be well-tightened and thoroughly oiled. The moulds were tested from a compressive testing machine of 2000 KN capacity after being permitted to cure for 28 days in a curing tank at standard temperature. The test procedure was used per IS 516 (Part-1 Sec-I) – 2021[57].

2.3 Taguchi: Design of experiments

In the early 1950s, Genichi Taguchi created Taguchi's Design of Experiments[59], a fractional factorial approach. Taguchi identifies the minimum orthogonal arrangement needed for the testing parameters for every experiment element, which requires fewer experimental runs than traditional factorial designs[60]. The Taguchi technique is a helpful tool for analysing impact factors using orthogonal arrays (OA) and figuring out the optimal combination of factor levels[61]. The OA is represented as $L_x(y^z)$, where x is the combination of factors, y is the total number of components' levels, and z is the total number of factors[61]. Conventional experimental design methods, such as full factorial designs, mainly focus on optimizing the mean value of the quality characteristic. In contrast, the use of orthogonal arrays helps minimize the variation in the quality characteristic, leading to more robust and consistent results[62]. The Taguchi approach uses the signal-to-noise (S/N) ratio during process optimization in place of the mean value to combine the experimental data into a single performance measure.The S/N ratio serves as a robustness metric by comparing the mean (signal) to the standard deviation (noise). It aids in identifying control factors that minimize the influence of uncontrollable variables and reduce overall process variability.The general definition of these quality attributes is that the smaller is better, the higher is better, or the nominal is best, and the goal value should be maintained[63]. Taguchi's design aims to decrease process standard deviation to increase product quality[64]. Main effect plots demonstrate how changes in control parameters affect the product's attributes. If the slope of the line is high, the factors have a considerable impact on the response, and a low line slope shows that the factors do not affect the response[65]. Fig. 6 shows the process involved in the Taguchi design of the experiment.

The S/N ratio with Nominal-is-best (Eq.1), larger-is-better (Eq.2), and Smaller-is-better (Eq.3) to evaluate minimum variance to obtain important factors[66].

$$\text{Nominal-is-best} = 10\ log\left(\frac{\bar{a}^2}{s^2}\right) \quad \ldots(1)$$

$$\text{Larger-is-better} = -10\ log\left(\frac{\sum_{i=1}^{n}\frac{1}{a_i^2}}{n}\right) \quad \ldots(2)$$

$$\text{Smaller-is-better} = -10\ log\left(\frac{\sum_{i=1}^{n} a_i^2}{n}\right) \quad \ldots(3)$$

Where n is the experimental trial number, s is the response's standard deviation, and a_i is the measured response value.

Six factors, i.e., Cement (OPC), Fine aggregates (FA), Coarse aggregates (CA), Metakaolin (MK), Polypropylene fiber (PPF), and water-cement ratio

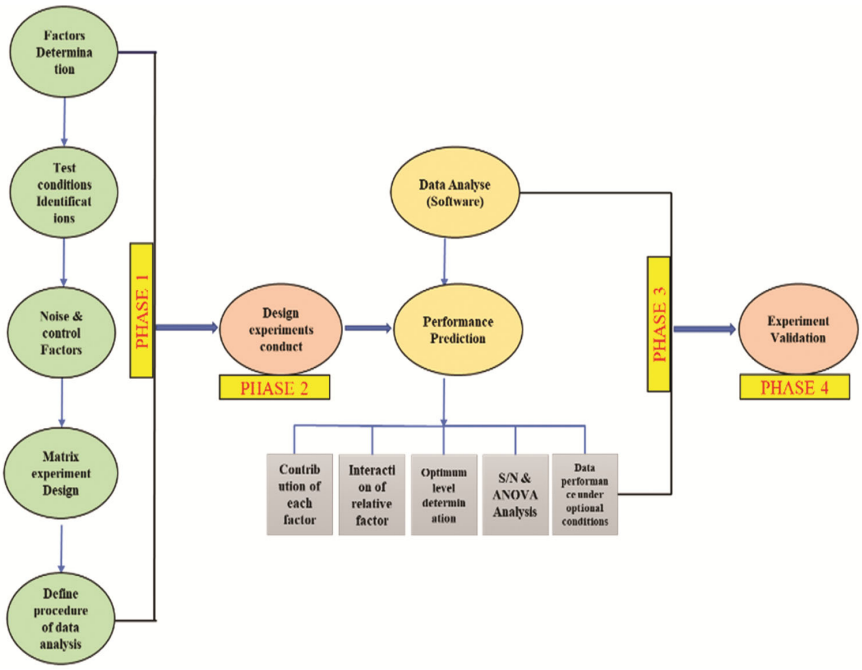

Fig. 6 — Taguchi method design of experiments.

(w/c ratio), each of which had five levels for MK/SF& PPF combination.

Twenty-five experimental series were designed based on a Taguchi O.A. L_{25} (5^6) in Table 5 to analyse the Workability, density, and mechanical properties of the MK/SF and PPF.

2.4 Analysis of variance (ANOVA)

Analysis of variance (ANOVA) was employed to quantify the impact of each factor on the response variables, and predictive models were developed expressing the responses as functions of these factors[67]. The terms D.F., M.S., and S.S. denote the degrees of freedom, mean of squares, and sum of squares, respectively. Table 6 shows the One-way ANOVA setup.

Where n = trials, $\overline{a}$ = target value

$$\left(\text{percentage of contribution} = \frac{\text{S. S.}}{\text{Sum of S. S.}} \text{ X } 100\right)$$

The area under the proper null-sampling distribution of the F-value is known as the *P*-value. The model characteristics are deemed significant if their p-values are smaller than 0.05. When the model terms exceed 0.10, they are deemed to be non-significant.

3 Results & Discussion

The strength characteristics of continuously cured concrete specimens were evaluated at 7 and 28 days. The next subsections present the mechanical properties at various curing days regarding the effect of the S/N ratio. Eq. 2 was used to estimate the S/N ratio of mechanical properties, workability, and density. Regression analysis is also used to identify the best combination and create a linear model of the data.

3.1 Workability

A slump test was performed to check the fresh concrete consistency. The findings of the tests are evaluated and presented in Fig. 7. The maximum slump measured in the control mix without PPF and Supplementary cementitious components was 80mm. Adding 1% PPF in MK and SF reduces the slump value from 18.75% and 25%, respectively, compared with the control mix.

Fig. 7 shows the workability of supplementary cementitious components (10%), and increasing amounts of PPF dosage (0.25 %, 0.50 %, 0.75 %, and 1.00 %) might induce lower workability and a harsher mix. Table 7 illustrates the significance of the input parameters for workability in response to S/N ratio. The PPF, cement, FA, and CA were considered control parameters to maximize workability.

The impact of each parameter on the evolution of workability is displayed in Fig. 8.The S/N ratiovary from 35.75 to 37.75 for the workability from the response results.

It was found that the following essential components are ordered based on importance for

Table 5 — Taguchi Orthogonal Array for mixed proportion (kg/m^3).

S. No.	Experimental Parameters						Cement	FA	CA	MK/SF	PPF	w/c Ratio
	A	B	C	D	E	F						
MS1	1	1	1	1	1	1	332.7	823.28	1043.16	37	0	149.7
MS2	1	2	2	2	2	2	332.7	822	1041.63	37	0.92	149.7
MS3	1	3	3	3	3	3	332.7	820.8	1040	37	1.84	149.7
MS4	1	4	4	4	4	4	332.7	819.6	1038	37	2.76	149.7
MS5	1	5	5	5	5	5	332.7	818.4	1037	35	3.68	147.1
MS6	2	1	2	3	4	5	332.7	823.28	1041.63	37	2.76	147.1
MS7	2	2	3	4	5	1	332.7	822	1040	37	3.68	149.7
MS8	2	3	4	5	1	2	332.7	820.8	1038	35	0	149.7
MS9	2	4	5	1	2	3	332.7	819.6	1037	37	0.92	149.7
MS10	2	5	1	2	3	4	332.7	818.4	1043.16	37	1.84	149.7
MS11	3	1	3	5	2	4	332.7	823.28	1040	35	0.92	149.7
MS12	3	2	4	1	3	5	332.7	822	1038	37	1.84	147.1
MS13	3	3	5	2	4	1	332.7	820.8	1037	37	2.76	149.7
MS14	3	4	1	3	5	2	332.7	819.6	1043.16	37	3.68	149.7
MS15	3	5	2	4	1	3	332.7	818.4	1041.63	37	0	149.7
MS16	4	1	4	2	5	3	332.7	823.28	1038	37	3.68	149.7
MS17	4	2	5	3	1	4	332.7	822	1037	37	0	149.7
MS18	4	3	1	4	2	5	332.7	820.8	1043.16	37	0.92	147.1
MS19	4	4	2	5	3	1	332.7	819.6	1041.63	35	1.84	149.7
MS20	4	5	3	1	4	2	332.7	818.4	1040	37	2.76	149.7
MS21	5	1	5	4	3	2	330	823.28	1037	37	1.84	149.7
MS22	5	2	1	5	4	3	330	822	1043.16	35	2.76	149.7
MS23	5	3	2	1	5	4	330	820.8	1041.63	37	3.68	149.7
MS24	5	4	3	2	1	5	330	819.6	1040	37	0	147.1
MS25	5	5	4	3	2	1	330	818.4	1038	37	0.92	149.7

Table 6 — One-way ANOVA setup.

Source of Variation	S.S.	D.F.	M.S.	F-ratio
Between categories or samples	$n_1(\overline{a}_1 - \overline{a})^2 + n_2(\overline{a}_1 - \overline{a})^2$ +……..+ $n_k(\overline{a}_j - \overline{a})^2$	$(j-1)$	$\frac{ss\ between}{(j-1)}$	$\frac{MS\ between}{MS\ within}$
Within categories or samples	$\sum(a_{1i} - \overline{a}_1)^2 + \sum(a_{2i} - \overline{a}_2)^2 +$ ……+ $\sum(a_{ji} - \overline{a}_j)^2$	$(n-k)$	$\frac{ss\ within}{(n-k)}$	
Total	$\sum_{i=1,2,3...\&j=1,2,3\ldots}(a_{ij} - \overline{a})^2$	$(n-1)$		

Table 7 — S/N ratio response for workability.

Level	Cement	FA	CA	MK/SF	PPF	Water
1	36.47	36.79	36.79	36.78	37.54	36.80
2	36.84	36.76	36.78	36.77	37.22	36.76
3		36.77	36.76		36.75	
4		36.78	36.77		36.44	
5		36.75	36.75		35.90	
Delta	0.37	0.04	0.04	0.01	1.64	0.03
Rank	2	3	4	6	1	5

reaching higher workability: cement (33.27 kg/m^3), FA (818.40 kg/m^3), CA (1037 kg/m^3), MK (35 kg/m^3), PPF (0 kg/m^3), and water (147.9 kg/m^3).Theeffects of each parameter on the continued development of higher workability can be determined within the given range using the selected levels and mix proportions. Eq. 4 provides the regression equation for workability.

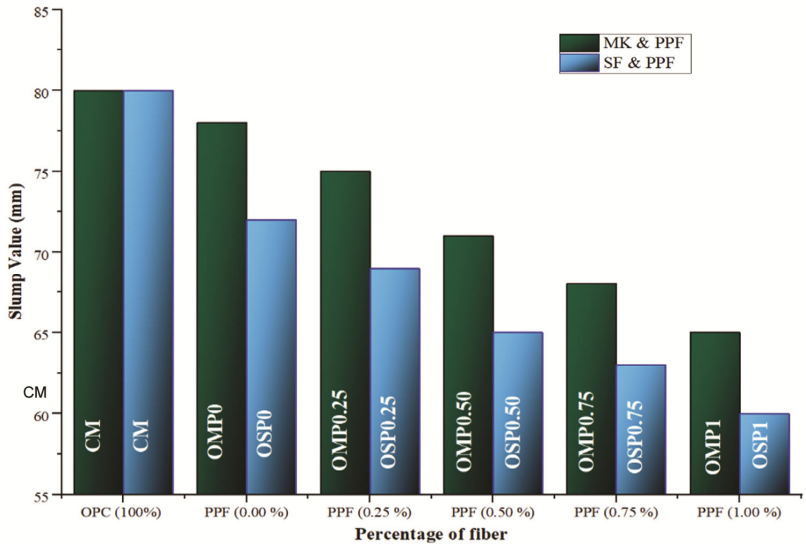

Fig. 7 — Workability of MK & PPF versus SF & PPF.

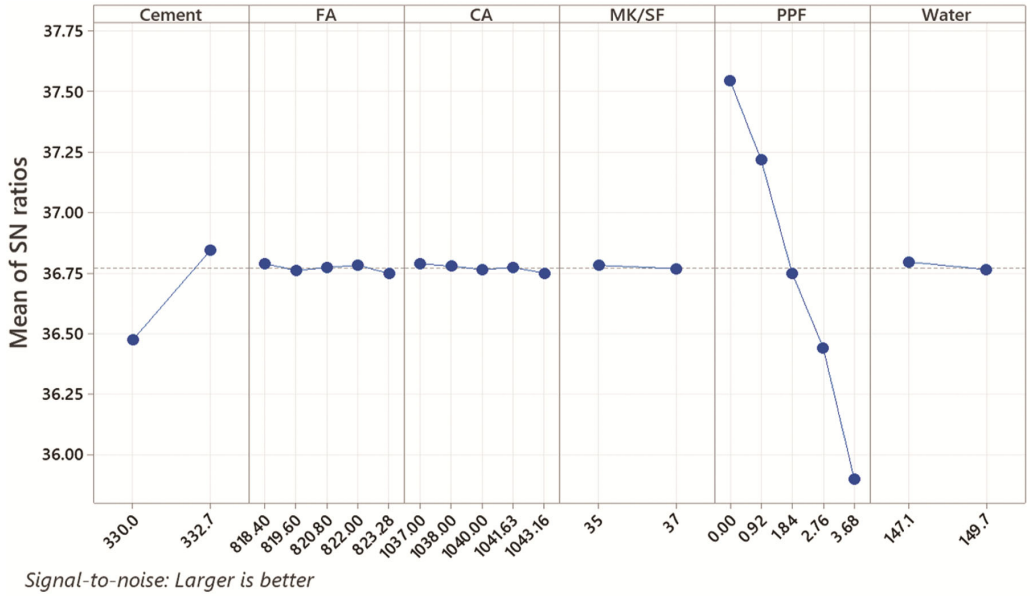

Fig. 8 — Main effect graph for S/N ratio on workability.

Workability = -233 + 1.074 Cement - 0.017 FA - 0.025 CA - 0.050 MK/SF - 3.500 PPF - 0.038 Water … (4)

The regression equation was generated from the Minitab 20.0 software using all of the provided input parameters. The Pareto chart of standardized effects for workability (Fig. 9a) illustrates the impact of various predictors on the response variable, with the standardized effects shown on the x-axis. Predictors such as cement (A) and PPF (E) have significant effects, as their bars exceed the critical value threshold (indicated by the red line at 2.10). This implies that changes in the amounts of cement and water significantly influence the workability of the concrete mix, with water showing the most substantial effect. Other predictors, such as FA (B), CA (C), MK/SF (D), and water (F), do not significantly affect workability, as their bars do not surpass the critical value threshold. Fig. 9(b) displays the typical probability plot curve. The remainders closely resemble the straight line in the normal probability plot of workability residuals (Fig. 9b), indicating that they are roughly normally distributed. The premise of normalcy is substantially satisfied, as demonstrated by

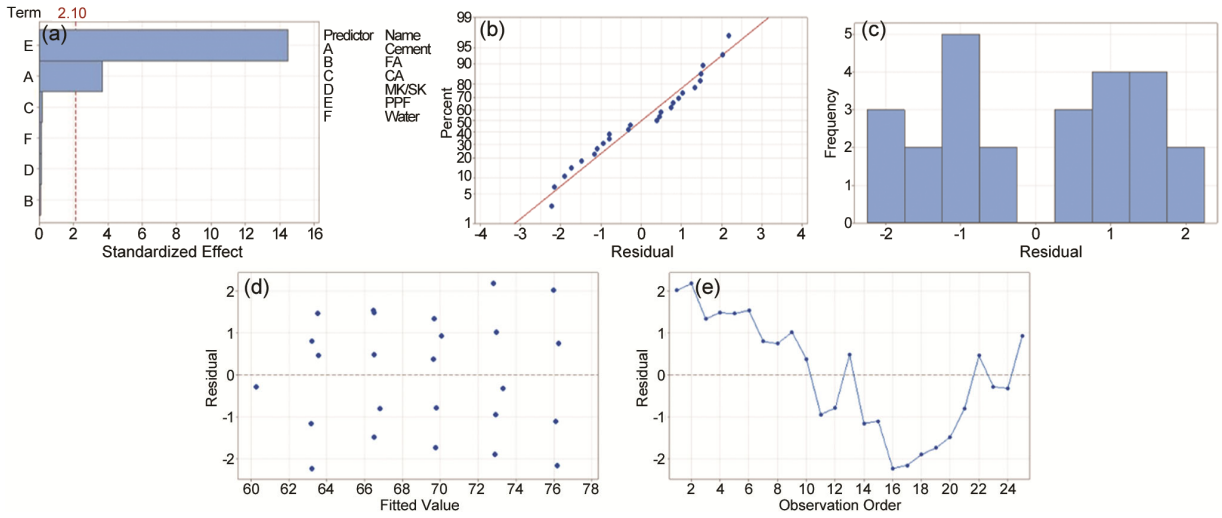

Fig. 9 —Residuals graphs for workability (a) Frequency order graph, (b) Normally distributed graph, (c) Histogram graph, (d) Fit versus residual graph, and (e) Order versus residual graph.

Table 8 — Analysis of variance for workability.

Source	D.F.	S.S.	M.S.	F-Value	P-Value	Percentage contribution
Regression	6	552.243	92.041	37.32	0.000	92.559
Cement	1	33.640	33.640	13.64	0.002	5.638
FA	1	0.021	0.021	0.01	0.927	0.004
CA	1	0.082	0.082	0.03	0.857	0.014
MK/SF	1	0.040	0.040	0.02	0.900	0.007
PPF	1	518.420	518.420	210.19	0.000	86.890
Water	1	0.040	0.040	0.02	0.900	0.007
Error	18	44.397	2.466			7.441
Total	24	596.640				100.000

this linear pattern, which is important for the reliability of the statistical analyses and conclusions derived from the model. Although there may be some little deviations or outliers shown by small deviations from the line at the ends, overall, the graph is consistent with the normally distributed model residuals. The distribution of residuals around the mean is displayed in the workability residuals histogram (Fig. 9c). Although there are observable peaks at -1 and 1, suggesting that the residuals are not normally distributed, the residuals are distributed about symmetrically around zero. This implies that although the model has a reasonable degree of accuracy, the residuals may contain a small amount of non-normality. Multiple peaks and gaps in the distribution may indicate interactions or underlying causes that the current model does not fully capture.

The residuals, or variations between observed and predicted values, are presented against the fitted values in the workability fitted graph (Fig. 9d). By looking for any patterns in the residuals, this graphic aids in determining whether the model is adequate. The residuals in this instance exhibit a random dispersion about the zero line with no apparent pattern, suggesting that the model's linearity and uniformity (constant variance) assumptions are probably satisfied. This randomness indicates no systematic bias in the residuals and that the model fits the data adequately. The residuals, or the disparities between observed and anticipated values, are shown against the observation order in the residuals against order plot (Fig. 9e) for workability. This plot helps identify any patterns or trends in the residuals over time, which can indicate non-randomness in the data. In this case, the residuals fluctuate around zero initially with a clear downward trend, followed by an upward trend, suggesting potential time-related effects or other systematic patterns affecting the workability measurements. This analysis indicates that further investigation may be required to identify and address any underlying causes of these trends.

Table 8 shows that the factor PPF has the maximum substantial contribution, followed by cement. All selected factors strongly support the null

hypothesis (i.e., that all level means are equal) when the P-value for any source is greater than 0.05.

3.2 Compressive strength

The study of compressive strength of concrete shows incorporating MK & PPF and MK & SF. In all specimens, the compressive strength increases as a partial replacement (10%) of MK and SF with cement.

The SF has greater compressive strength than MK, 3.53% and 12.25% observed on 7 and 28 days of curing, respectively. While MKwas partially replaced with cement, the compressive strength increased by 33.11% and 15.41% on the 7 and 28 days of curing, respectively, in contrast to the control mix design. For SF (10%), the compressive strength increases by 37.82% and 29.55% on 7 and 28 days, respectively. While increasing the PPF dosage, considerable improvement in compressive strength was not observed, as shown in Fig. 10 and 11.

Table 9 illustrates the significance of the contribution parameters for 28 days of compressive strength in response to S/N ratio. The PPF, cement, CA, and FA were considered control parameters to maximize compressive strength. The effect of each parameter on the compressive strength development is illustrated in Fig. 12.The S/N ratio vary from 30.50 to 31.50 for the response results.

The components ranked by their importance for achieving maximum compressive strength (Table 9)

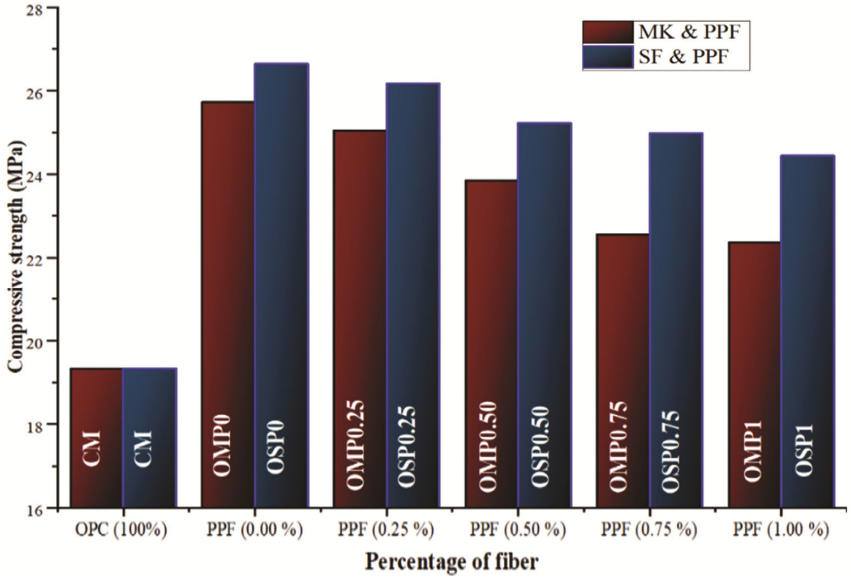

Fig. 10 — Comparison of compressive strength of MK & PPF versus SF & PPF concrete mixes at 7 days.

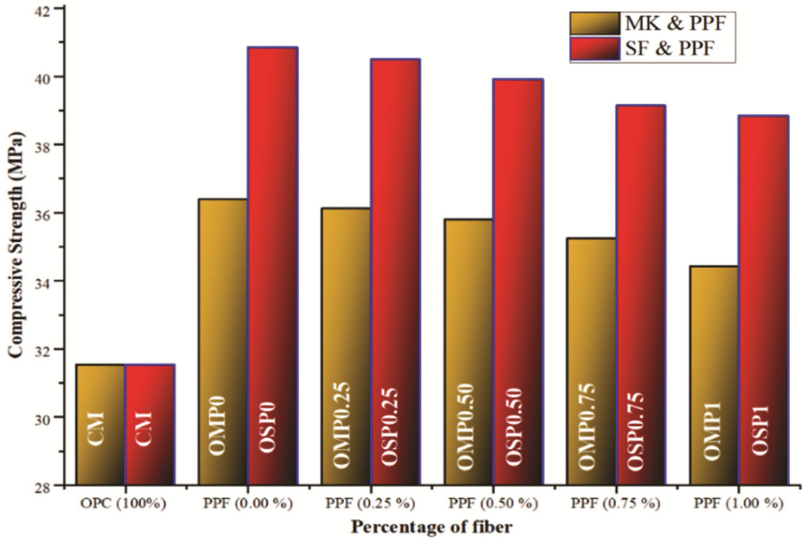

Fig. 11 — Comparison of compressive strength of MK & PPF versus SF & PPF concrete mixes at 28 days.

Table 9 — S/N ratio response for compressive strength.

Level	Cement	FA	CA	MK/SF	PPF	Water
1	31.00	31.02	31.01	31.01	31.21	31.01
2	31.02	31.01	31.01	31.01	31.14	31.01
3		31.01	31.02		31.05	
4		31.01	31.01		30.93	
5		31.01	31.01		30.72	
Delta	0.02	0.01	0.01	0.00	0.49	0.00
Rank	2	4	3	1	6	5

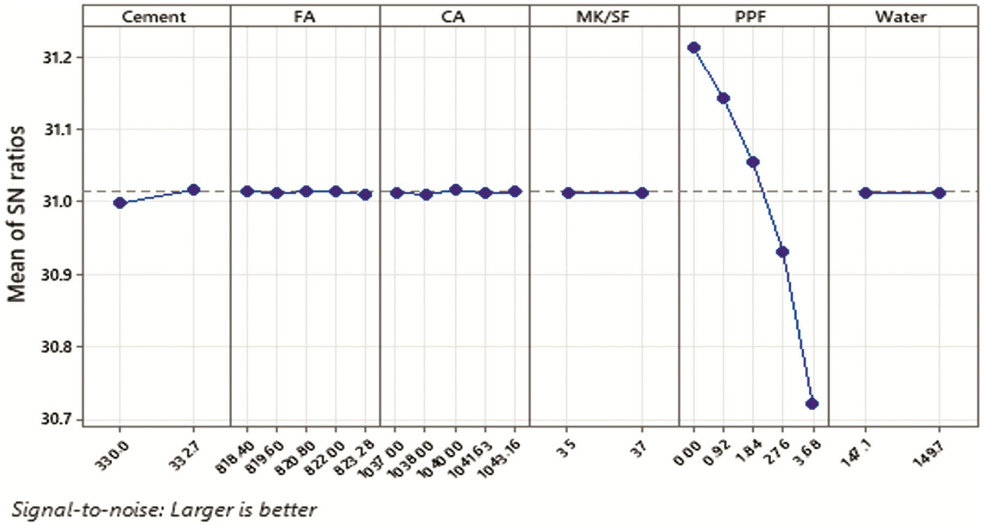

Fig. 12 — Main effect plot for S/N ratio on compressive strength.

are as follows: Cement (33.27 kg/m³), FA (822 kg/m³), CA(1040 kg/m³), MK/SF (35 kg/m³), PPF (0 kg/m³), and Water (147.1 kg/m³). It is important to remember that, within the given range, the levels and mix proportions selected can be used to determine the effects of each parameter on the ongoing search for improved compressive strength. Eq. 5 shows the regression eq. for compressive strength.

$$\text{Compressive Strength} = 27.3 + 0.0285\ \text{Cement} - 0.0027\ \text{FA} + 0.0015\ \text{CA} - 0.0003\ \text{MK/SF} - 0.5283\ \text{PPF} + 0.0027\ \text{Water} \quad \ldots (5)$$

The proportional importance of several predictors on compressive strength is displayed in the ordered frequency chart of standardized effects (Fig. 13a) with an alpha level of 0.05. In this chart, the predictors are Cement (A), FA (B), CA (C), MK/SF (D), PPF (E), and Water (F). The chart indicates that MK/SF (D) has the most significant effect, far exceeding the critical value (2.10) for statistical significance.

Cement (A) also shows a notable effect, but is less impactful than MK/SF. Other predictors, such as FA, CA, PPF, and Water, show an significant minimal impact. This suggests that including MK/SF and Cement is critical in enhancing compressive strength, while the other components play a smaller role. The normal probability plot illustrates the compressive strength residuals' normal distribution (Fig. 13 b). The plot shows that the residuals are roughly normally distributed since most pointsnearly resemble a straight line. But there are some discrepancies in the tails, especially around the bottom end, which point to minor differences from ordinary. These deviations are not severe enough to question the model's overall validity. Therefore, the assumption of normality for the residuals holds reasonably well, supporting the consistency of the regression model in forecasting compressive strength with acceptable accuracy. The histogram of residuals for compressive strength shows the distribution of residuals around the zero line. The residuals are distributed symmetrically, as the histogram (Fig. 13c) shows peaks at -0.12 and 0.12. This suggests that the majority of residuals are close to zero. This symmetry and the bell-shaped distribution indicate that the residuals are nearing a

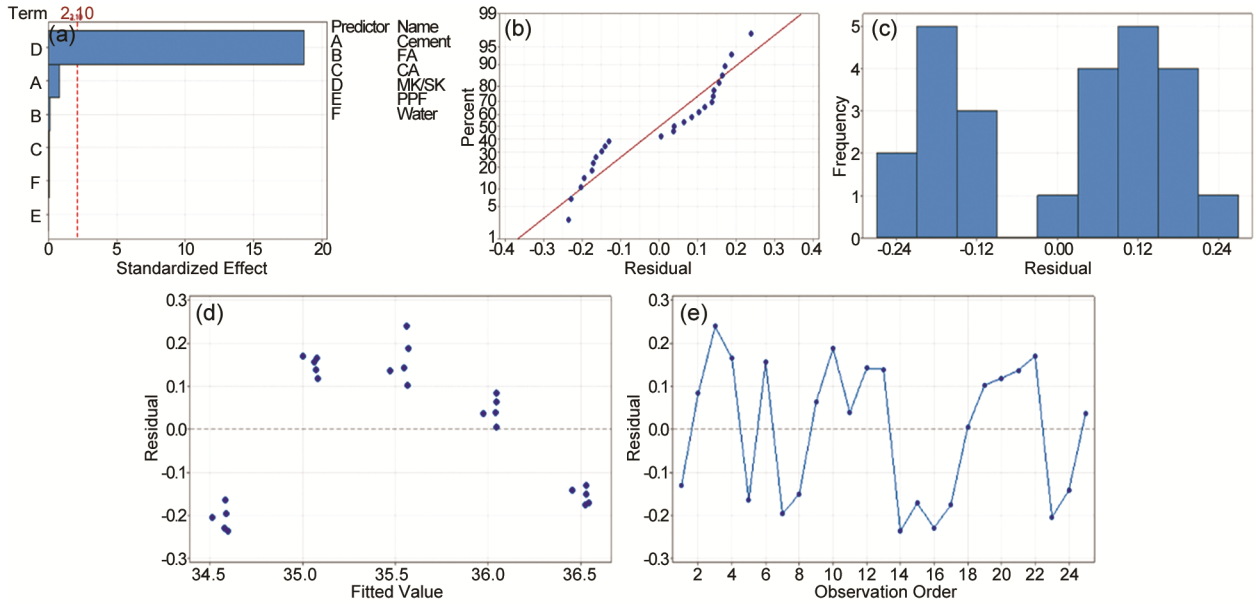

Fig. 13 — Residuals graphs for compressive strength (a) Frequency order graph, (b) Normally distributed graph, (c) Histogram graph, (d) Fit versus residual graph, and (e) Order versus residual graph.

Table 10 — Analysis of Variance for compressive strength.

Source	D.F.	S.S.	M.S.	F-Value	P-Value	Percentage contribution
Regression	6	11.8345	1.9724	58.56	0.000	95.127
Cement	1	0.0237	0.0237	0.70	0.412	0.191
FA	1	0.0005	0.0005	0.02	0.902	0.004
CA	1	0.0003	0.0003	0.01	0.928	0.002
MK/SF	1	0.0000	0.0000	0.00	0.996	94.928
PPF	1	11.8098	11.8098	350.64	0.000	0.000
Water	1	0.0002	0.0002	0.01	0.940	0.002
Error	18	0.6063	0.0337			4.873
Total	24	12.4408				100.000

normal distribution, which supports the normality assumption of the regression model.

Such a distribution implies that the model accurately captures the data's variability and that no significant biases or outliers affect the compressive strength estimations. This validation of the model's basic assumptions reinforces the model's robustness and dependability in compressive strength forecasts based on the variables under examination. The "Residuals versus Fits" images (Fig. 13d) for compressive strength show the residuals compared to the regression model's fitted values. The figure is essentially a random distribution of points around the zero line with no evident pattern or trend. This unpredictability suggests that the residuals have constant variance, and the model does not include any significant biases, giving the data a good fit.

The linearity and homogeneity assumptions are most likely met because there isn't a noticeable pattern, indicating that the regression model's analysis of the compressive strength data is valid. This figure proves the model can estimate compressive strength based on the parameters. The observation plot (Fig. 13e) for compressive strength displays the residuals from the regression analysis against the observation order. The plot shows a fluctuating pattern of residuals around the zero line, indicating no apparent trends or systematic errors over time. The random distribution of the residuals indicates that the errors are independent and the model fits the data adequately. From Table 10, it is observed that the factor MK/SF has the maximum substantial contribution.

3.3 Flexural strength

From experimental data, it was analysed that the maximum flexural strength was observed at 0.50% PPF dosage for both mix design specimens. SF & PPF have more flexure strength (12.25%) than MK & PPF

specimens at 0.50% PPF dosage.The flexural strength was enhanced by 25% and 34% at 0.50% PPF dosage for MK & PPF and SF & PPF, respectively, compared to the control mix design. After increasing the PPF dosage, there is a slight increase in flexural strength at a maximum of 1% PPF dosage, as shown in Fig. 14.

Table 11 illustrates the consequence of the input parameters for flexural strength in response to S/N ratio. To maximize flexural strength, the PPF, cement, CA, and FA were considered in ascending order, as control parameters. The impact of each criterion on the evolution of flexural strength is illustrated in Fig. 15. The S/N ratio vary from 11.40 to 13.00 for

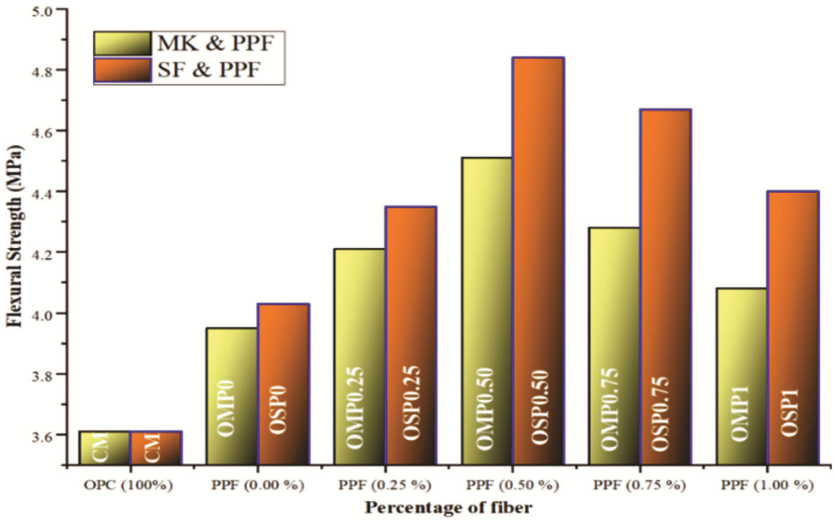

Fig. 14 — Flexural strength of MK & PPF versus SF & PPF.

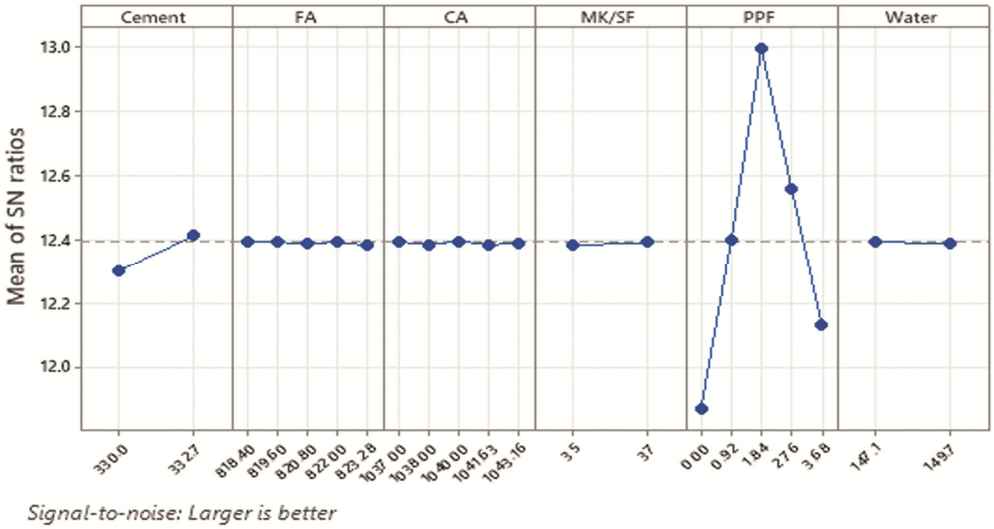

Fig. 15 — Main effect graph for S/N ratio on Flexural strength.

Table 11 — S/N Ratio response for flexural strength.

Level	Cement	FA	CA	MK/SF	PPF	Water
1	12.30	12.39	12.40	12.38	11.87	12.39
2	12.41	12.39	12.39	12.39	12.40	12.39
3		12.39	12.40		12.99	
4		12.39	12.39		12.56	
5		12.38	12.39		12.13	
Delta	0.11	0.01	0.01	0.01	1.12	0.00
Rank	2	3	4	5	1	6

the flexural strength from the response results. It was found that the following essential components are ordered based on importance for reaching maximum compressive strength: cement (33.27 kg/m^3), FA (822 kg/m^3), CA (1040 kg/m^3), MK (37 kg/m^3), PPF (1.84 kg/m^3), and water (147.1 kg/m^3).

The Main Effects plot for the S/N ratio (Fig. 15) illustrates the influence of key factors, such as water, cement, FA, CA, MK/SF, and PPF, on the response variable.The S/N ratio, where "larger is better," indicates that the higher values represent improved performance. The plot reveals that Cement, FA, CA, MK/SF, and Water have relatively consistent effects on the response, showing minimal variation across their levels. However, PPF displays significant variation, with the mean S/N ratio peaking sharply at 1.84 and dipping at other levels. This indicates that including PPF at specific levels substantially impacts the response, highlighting its critical role in enhancing the material's performance. The data suggests that careful adjustment of PPF levels could optimize the response, while the other factors maintain more stable contributions.

It is important to note that, within the specified range, the selected levels and mix proportions enable the evaluation of each parameter's effect to enhance the flexural strength.Eq. 6 provides the regression equation for an optimum combination of flexural strength.

$$\text{Flexural Strength} = -1.4 + 0.0196\ \text{Cement} - 0.0010\ \text{FA} - 0.0002\ \text{CA} + 0.0027\ \text{MK/SF} + 0.0346\ \text{PPF} - 0.0008\ \text{Water} \quad \ldots (6)$$

The Pareto chart of standardized effects for the response variable flexural strength (Fig. 16a) identifies the most significant factors influencing the response. The chart shows that PPFhas the most important standardized effect, followed by Cement. These factors surpass the significance threshold marked by the red dashed line at 2.101, indicating their substantial impact on flexural strength. Other variables that do not exceed the limit include FA, CA, MK/SF, and Water, suggesting that their effect on the flexural strength in this investigation is not as significant. This demonstrates how vital PPF and cement are in raising the material's flexural strength and implies that adjusting these constituents' quantities might significantly enhance the end product's performance.The standard probability plot shows the degree to which the residuals for flexural strength follow a normal distribution (Fig. 16b). The residuals may be roughly normally distributed if the points generally follow a straight line.At the lower and upper ends, in particular, a few locations deviate from the line, causing some variations at the tails. This modest divergence from normalcy can point to some outliers or variability that the model cannot adequately account for. The plot indicates that the residuals' normality assumption is quite valid; however, additional model adjustment would be required to account for the observed deviations.

The residuals histogram (Fig. 16c) indicates that the model tends to somewhat overpredict flexural strength, with most residuals being grouped around the mean and a clear skew towards negative values. The fact that there are residuals on both sides of the mean indicates that the model is not significantly biased. The distribution is not exactly symmetrical, though, which can point to some underlying variability in the information or flaws in the model.

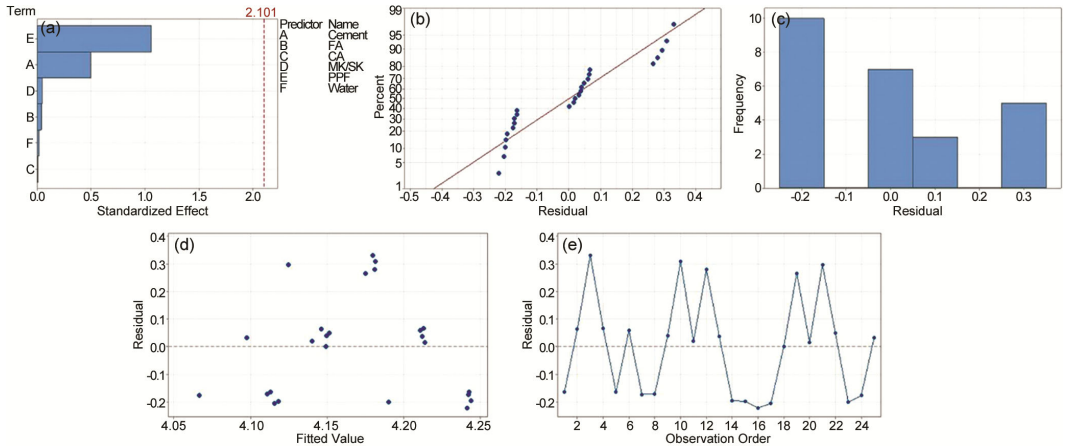

Fig. 16 — Residuals graphs for compressive strength (a) Frequency order graph, (b) Normally distributed graph, (c) Histogram graph, (d) Fit versus residual graph, and (e) Order versus residual graph.

The histogram indicates regions that could be improved for increased accuracy but indicates that the model does a fair job of predicting flexural strength.The residuals in flexural strength are plotted against the fitted values in the fitted plot (Fig. 16d) to evaluate the correctness of the model and spot any trends or discrepancies.The fact that the residuals are dispersed and lack a clear pattern suggests that they are randomly distributed.This unpredictability implies no systematic mistakes in the fitted values, hence supporting the validity of the model's assumptions.

However, the scatter in residual values and the existence of some clusters draw attention to possible data variability that may result from inherent material characteristics or experimental setup.

The observation plot (Fig. 16e) for residuals in flexural strength displays the residuals against the observation order to identify any patterns or anomalies over time. The plot exhibits fluctuations in residuals, with peaks reaching approximately 0.4 and troughs around -0.2. These variations suggest the presence of some cyclical patterns, indicating possible non-randomness in the residuals. The absence of a clear trend or systematic pattern across the observation order implies that the model fits the data reasonably well, although some observations deviate more significantly than others. From Table 12, it is observed that the factor PPF has the maximum substantial contribution.

3.4 Splitting tensile strength

From experimental results, it was observed that the maximum tensile strength was observed at 0.75% PPF dosage for both mix design specimens. SF & PPF have more tensile strength (4%) than MK & PPF specimens at 0.75% PPF dosage. Compared to the control mix design, the tensile strength was enhanced by 36% and 41.78% at 0.75% PPF dosage for MK & PPF and SF & PPF, respectively. After increasing the PPF dosage, there is a slight increase in flexural as shown in Fig 17. The S/N ratio vary from 10.00 to 12.00 for the splitting tensile strength from the response results. The S/N ratio vary from 10.00 to 12.00 for the splitting tensile strength from the response results. It was found that the following essential components are ordered based on importance for reaching maximum splitting tensile

Table 12 — Flexural strength variance analysis.

Source	D.F.	S.S.	M.S.	F-Value	P-Value	Percentage contribution
Regression	6	11.8345	1.9724	58.56	0.000	7.112
Cement	1	0.0237	0.0237	0.70	0.412	1.289
FA	1	0.0005	0.0005	0.02	0.902	0.008
CA	1	0.0003	0.0003	0.01	0.928	0.001
MK/SF	1	0.0000	0.0000	0.00	0.996	0.014
PPF	1	11.8098	11.8098	350.64	0.000	5.798
Water	1	0.0002	0.0002	0.01	0.940	0.002
Error	18	0.6063	0.0337			92.858
Total	24	12.4408				99.970

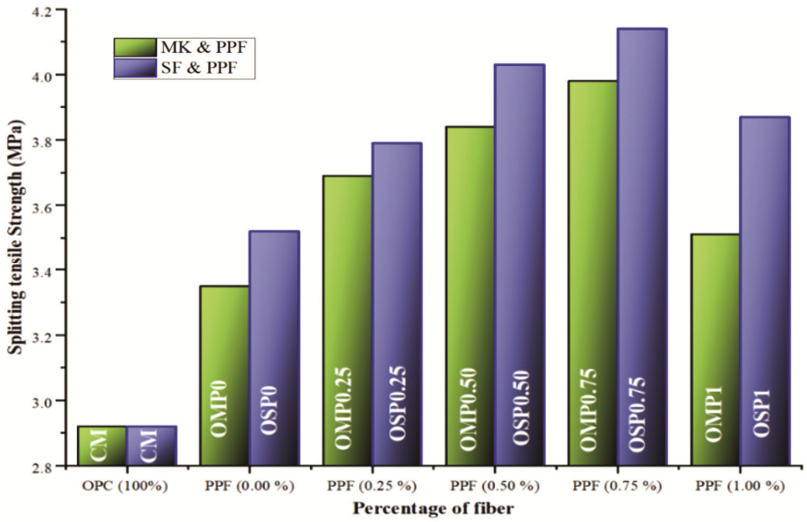

Fig. 17 — Splitting Tensile Strength of MK & PPF versus SF & PPF.

strength: cement (33.27 kg/m3), FA (822 kg/m3), CA (1040 kg/m3), MK (37 kg/m3), PPF (2.16 kg/m3), and water (147.1 kg/m3).

The main effect plot for S/N ratio on splitting tensile strength (Fig. 18) reveals that the addition of PPF has the most significant impact on S/N ratio, showing a pronounced increase in mean S/N ratio at higher PPF levels, indicating a strong positive effect on the response variable. Table 13 shows the S/N ratio response for splitting tensile strength.

In contrast, the factors Cement, FA, CA, MK/SF, and Water demonstrate relatively consistent mean S/N ratio across their respective levels, suggesting a minimal influence on the response variable. This indicates that among the factors studied, PPF is the most influential in improving the response, while the other factors contribute less significantly to variations in S/N ratio.Eq. 7 provides the regression equation for an optimum combination of splitting tensile strength that has been calculated-

Splitting tensile strength = -6.1 + 0.0287 Cement - 0.0000 FA + 0.0002 CA + 0.0000 MK/SF+ 0.0657 PPF - 0.0010 Water … (7)

PPF and cement have the most significant standardized effects, according to the Pareto chart of the standardized impacts for splitting tensile strength (Fig. 19a), indicating that these two variables are essential for maximizing splitting tensile strength in the setting under study. Other factors, including FA, CA, MK/SF, and Water, exhibit minimal standardized effects, implying their lesser influence on the response variable. This analysis emphasizes how important it is to provide PPF and cement first priority while designing mixtures in order to optimize the splitting tensile strength of concrete applications. The residuals for splitting tensile strength show a nearly linear pattern along the red reference line in the standard probability plot (Fig. 19b), indicating that the residuals are normally distributed. The majority of the points are around the line, confirming the residuals' assumed normality. In order to validate the model and guarantee the precision and dependability of statistical conclusions, this alignment with the normal distribution is essential. The little deviations from this line confirm to the errors' symmetric distribution and lack of apparent skewness or kurtosis. Because the

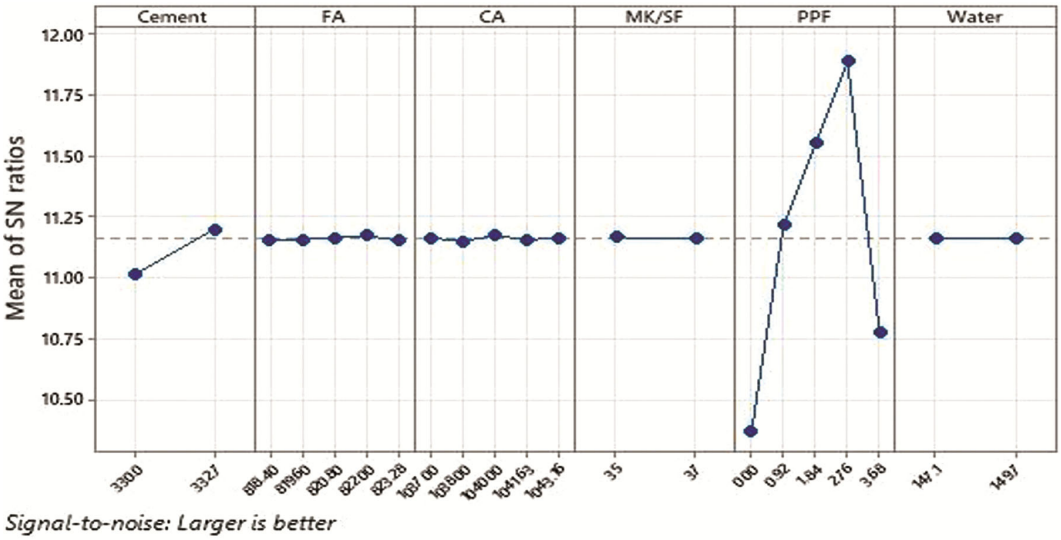

Fig. 18 — Main effect graph for S/N ratio on splitting tensile strength.

Table 13 — S/N Ratio response for splitting tensile strength.

Level	Cement	FA	CA	MK/SF	PPF	Water
1	11.01	11.16	11.16	11.17	10.38	11.16
2	11.20	11.16	11.15	11.16	11.22	11.16
3		11.16	11.17		11.55	
4		11.17	11.16		11.89	
5		11.15	11.17		10.78	
Delta	0.19	0.02	0.02	0.01	1.51	0.00
Rank	2	4	3	5	1	6

residuals are normal, the model's predictions for splitting tensile strength can therefore beregarded as reliable and solid. The distribution of residuals and the frequency at which each residual value occurs are displayed in the histogram of the residuals (Fig. 19c) for splitting tensile strength. The residuals show a symmetric distribution around zero, suggesting that the errors are dispersed uniformly and that the model's predictions are not systematically biased. With fewer data at the extremes, the majority of residuals are grouped around the centre, indicating a nearly normal distribution. This pattern ensures the validity of inferences derived from the model and supports the assumption of normality of errors, which is an essential requirement for many statistical analyses.

The residuals plot (Fig. 19d) displays no discernible pattern, which suggests that the variance of the errors is constant. The residuals fluctuate randomly around the zero line, showing that the predictions are unbiased. However, the spread of residuals at different levels of the fitted values should be further examined to ensure there are no underlying issues, such as non-linearity or omitted variables, which could affect the reliability and accuracy in predicting splitting tensile strength. The Observation plot (Fig. 19e) displays the residuals, implying that the model's assumptions about the independence of errors are likely valid.However, the variability in the residuals, with peaks and troughs, suggests some observations deviate more than others from the predicted values.These fluctuations highlight the need for careful examination of model adequacy and potential areas for improvement in predicting splitting tensile strength. From Table 14, it is observed that the factor PPF has the maximum substantial contribution (14.16%).

3.5 Density

The average density test results were performed on hardened concrete samples at 28 days, conforming to ASTM C642. This test method helps gather the data needed to convert concrete's mass and volume. It can determine accordance with concrete specifications and show differences from place to place within a concrete mass. The density was lower than the control

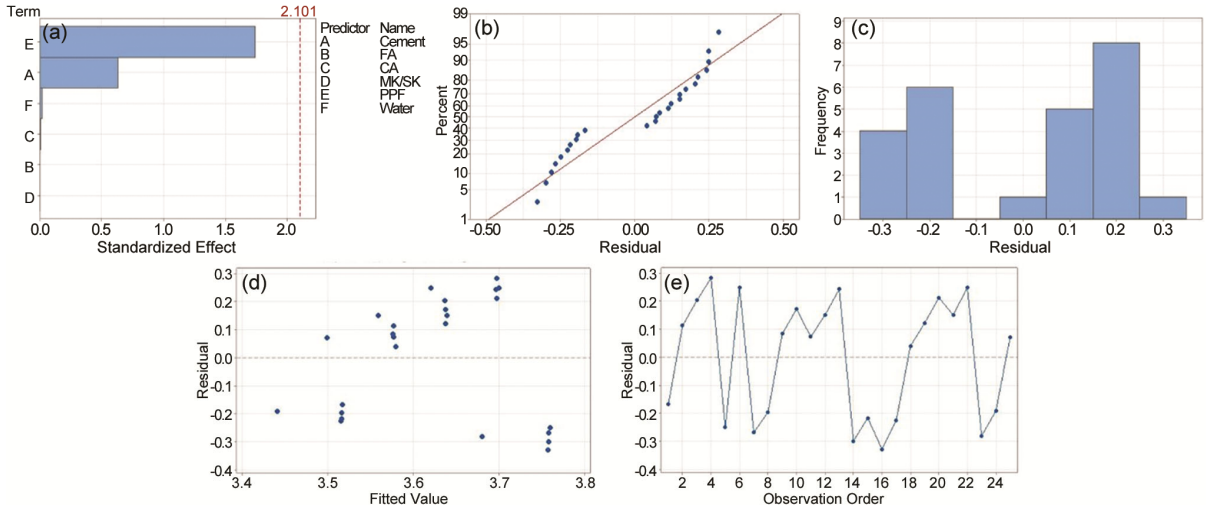

Fig. 19 — Residuals graphs for splitting tensile strength (a) Frequency order graph, (b) Normally distributed graph, (c) Histogram graph, (d) Fit versus residual graph, and (e) Order versus residual graph.

Table 14 — Splitting tensile strength variance analysis.

Source	D.F.	S.S.	M.S.	F-Value	P-Value	Percentage contribution
Regression	6	0.20646	0.034410	0.57	0.747	16.022
Cement	1	0.02403	0.024025	0.40	0.535	1.865
FA	1	0.00000	0.000000	0.00	0.999	0.000
CA	1	0.00000	0.000004	0.00	0.993	0.000
MK/SF	1	0.00000	0.000000	0.00	1.000	0.000
PPF	1	0.18241	0.182408	3.03	0.099	14.156
Water	1	0.00003	0.000025	0.00	0.984	0.002
Error	18	1.08214	0.060119			83.978
Total	24	1.28860				100.000

specimen's whenever coarse aggregate reduction occurred, as shown in Fig. 20. CA has significant impact on material mass than PPF. PPF mass is negligible compared to aggregate mass.The decrease in density with MK & PPF was observed 6.75% in contrast to the control mix design, and for SF & PPF, 8.04% was observed.

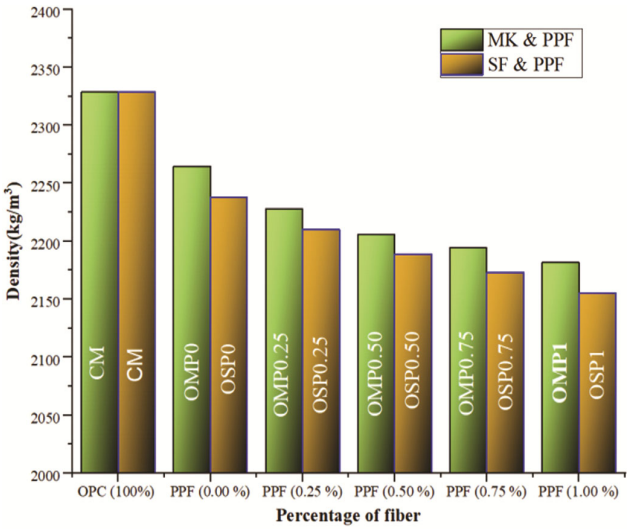

Fig. 20 — Density for MK & PPF versus SF & PPF.

Table 15 illustrates the significance of the input parameters for density in response to S/N ratio. To maximize density, the PPF, cement, CA, and FA were considered as control parameters. The impact of each parameter on the evolution of density is illustrated in Fig. 21. The S/N ratio vary from 66.75 to 67.10 for the density from the response results.

It was found that the essential components are ordered based on importance for reaching maximum splitting tensile strength: cement (33.27 kg/m3), FA (823.28 kg/m3), CA (1037 kg/m3), MK (37 kg/m3), PPF (0.00 kg/m3), and water (147.1 kg/m3).

It is important to remember that the levels and mix proportions chosen can be operated within the specified range to ascertain the impact of each parameter on the continuous demand for increased density. Eq. 8 provides the regression equation for an optimum combination of density.

$$\text{Density} = 1267 + 3.73\ \text{Cement} + 0.06\ \text{FA} - 0.346\ \text{CA} + 1.13\ \text{MK/SF} - 21.22\ \text{PPF} + 0.07\ \text{Water} \quad \ldots (8)$$

The Pareto Chart of the Standardized Effects (Fig. 22a), focusing on density as the response variable, highlights the relative impact of various predictors. The chart shows that PPF (E) has the most

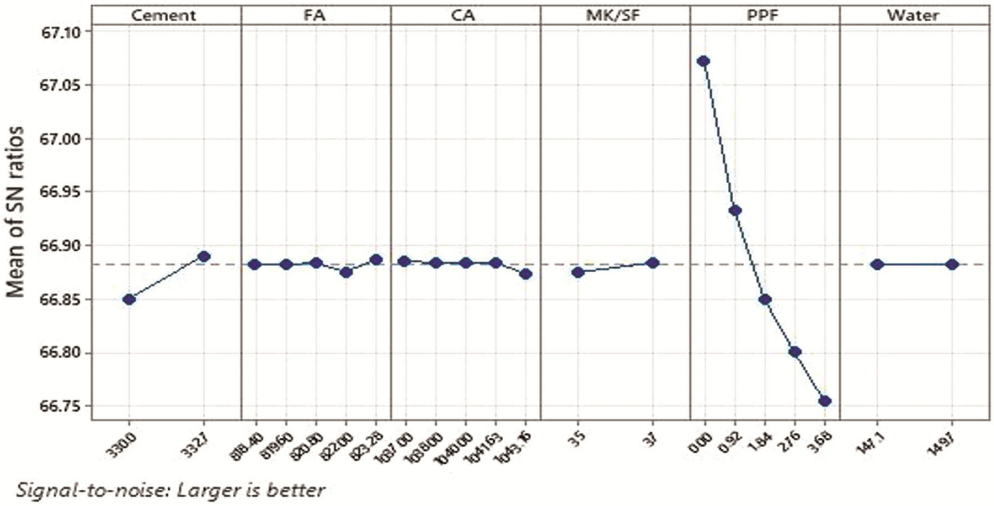

Fig. 21 — Main effect plot for S/N ratio on density.

Table 15 — S/N Ratio response for density.

Level	Cement	FA	CA	MK/SF	PPF	Water
1	66.85	66.88	66.89	66.87	67.07	66.88
2	66.89	66.88	66.88	66.88	66.93	66.88
3		66.88	66.88		66.85	
4		66.88	66.88		66.80	
5		66.89	66.87		66.76	
Delta	0.04	0.01	0.01	0.01	0.32	0.00
Rank	2	4	3	5	1	6

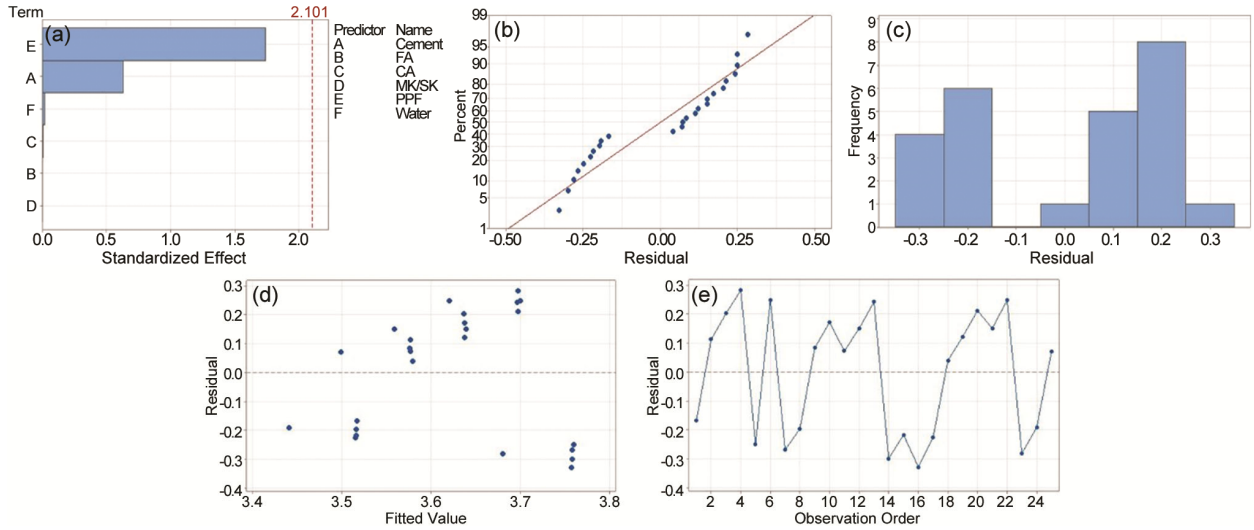

Fig. 22 — Residual plots for density (a) Pareto chart, (b) Normal probability plot, (c) Histogram, (d) Fitted curve, and (e) Observation plot.

critical effect on density, followed by Cement (A). Both factors exceed the significance threshold of 2.10, indicating a substantial influence on density. The other factors, FA, CA, MK/SF, and Water, have minimal effects, falling below the significance threshold. This analysis underscores the crucial role of PPF and Cement in determining the density of the concrete mix, suggesting that adjustments in these components can significantly alter the mix's density. The normality of the residuals is assessed using the standard probability plot of residuals for density (Fig. 22b). If the residuals are normally distributed, the points in this plot should form a straight line since the residuals are plotted against a hypothetical normal distribution.

The residuals follow a normal distribution, as seen by the points' substantial adherence to the diagonal reference line. On the lower end (harmful residuals), where a few points are farther from the line, there are some deviations near the tails. This shows that even if the residuals have an essentially normal distribution, there are a few outliers that could undermine the normalcy assumption. Overall, this plot supports the model's assumptions but also indicates areas where the model's fit could be improved.

The density histogram (Fig. 22c) displays the distribution of the variances between the observed and anticipated values. Residuals range from approximately -12 to +16, with a peak frequency around -4. The distribution appears to be slightly left-skewed, as more residuals are concentrated on the negative side, indicating a potential underestimation in the model's predictions. The spread of residuals suggests variability in prediction accuracy, with most residuals falling between -8 and +8. The presence of a few high positive residuals indicates specific instances where the model significantly overestimated the density. The fitted residuals curve (Fig. 22d) is randomly scattered around the zero line, showing no clear pattern, which suggests that the model assumptions are valid, particularly the assumption of homoscedasticity.

The fitted values range from approximately 2150 to 2250, with residuals varying from -10 to +15, indicating generally accurate predictions but with some deviations. The graph shows the residuals versus observation order for the response variable, which is density. The observation plot (Fig. 22e) is used to check for any patterns in the residuals, which would indicate potential problems with the model, such as non-randomness, trends, or systematic errors.

In this graph, the residuals fluctuate around zero, indicating that the model's errors are randomly distributed. The lack of clear trends or patterns suggests that the model does a good job of fitting the data. However, there are some points with relatively high residuals, both positive and negative, indicating a few observations where the model's predictions were less accurate. This analysis suggests that while the model generally performs well in predicting density, there are specific observations where the predictions deviate more significantly from the actual values. From Table 16, it is observed that the factor PPF has the maximum substantial contribution followed by cement. Fig. 23 shows the experimental process of the concrete mixture.

Table 16 — Density variance analysis.

Source	D.F.	S.S.	M.S.	F-Value	P-Value	Percentage contribution
Regression	6	19495.5	3249.3	38.03	0.000	92.689
Cement	1	406.3	406.3	4.76	0.043	1.932
FA	1	0.3	0.00	0.956	0.3	0.001
CA	1	15.4	15.4	0.18	0.676	0.073
MK/SF	1	20.4	20.4	0.24	0.631	0.097
PPF	1	19053.1	19053.1	223.02	0.000	90.585
Water	1	0.1	0.1	0.00	0.969	0.000
Error	18	1537.8	85.4			7.311
Total	24	21033.3				100.000

Fig. 23 — Experimental Process (a) Slump test, (b) Preparation of samples, (c) Curing of samples, (d) weight of cubes for density, (e) Cube test on compressive testing machine, (f) Cylinder test on compression testing machine, and (g) Testing of beam on flexural testing machine.

According to IRC:44-2017[68] and stated in a previous study[69–71], concrete with flexural and compressive strength of more than 3.8 and 30 MPa, respectively, concerning curing of 28 days, is considered suitable for rural roads in rigid pavement construction. Further, the concrete with 4.5 and 40 MPa of flexural and compressive strength, respectively, corresponding to curing of 28 days, is considered suitable concrete pavement construction for urban roads. From the above-obtainedresults, it is clear that cement replacement with SF without PPF can be used for rigid pavement construction on both rural and urban roads. From the above results, Partial replacement of SF and MK with 0.50% dosage of PPF gives higher flexural strength, which is required for urban and rural concrete road pavement.

4 Conclusion

This study compares the MK & PPF v/s SF & PPF effect on the concrete`s mechanical properties. From the experimental and analytical results, the following important conclusions are made-

1 The cement ispartially replaced by MK and SF (10%). The PPF dosageis increased from 0.25 to 1% in both samples. As the cement was partially replaced with SCMs and the PPF dosage increased, the workability decreased for both samples. The reduction in workability was more significant in SF & PPF than in MK & PPF samples. This indicates that when the PPF dosage increases, concrete prepared from SF produces a harsher mix than MK concrete.

2 As the cement is partially replaced with MK & SF, the compressive strength increases because MK & SF particles are finer than Portland cement. The compressive strength for SF at 10% replacement was increased by 12.25% compared to MK atthe exact dosage. However, a 29.5% increasewas observed compared to the control mix. Increasing the dosage of PPF does not show

a considerable improvement in compressive strength for both SF and MK.

3 Replacing a portion of cement with MK or SF is suitable for rigid pavements that must open to traffic quickly, because both mixes reach more than 20 MPa compressive strength at 7 days.

4 The flexural strength is observedto be maximum at 0.50% PPF dosage for both MK and SF specimens. The flexural strength for SF is 7.32% more than MK at a 0.50% dosage of PPF. However, a 34% increase was observed compared to the control mix.

5 The splitting tensile strength is observed to be maximum at 0.75% PPF dosage for MK and SF specimens. The splitting tensile strength for SF is 4.02% more than that of MK at a 0.75% dosage of PPF. However, a 38% increase was observed compared to the control mix.

6 The density of specimens decreases with increasing PPF dosage. The reduction in density with MK & PPF was observed at 6.75% in contrast to the control mix design, and for SF & PPF, 8.04% was observed. The decrease in density was observed to begreater in SF than in MK.

7 Taguchi and multi-regression analysis results show that PPF content is the main factor for flexural and tensile strength, whereas MK and SF are the key factors for compressive strength.

This study concluded that the cement is partially replaced by SF and MK with a 0.50% dosage of PPF, which is found to be a suitable, cost-effective, and novel material, minimizing waste disposal problems incorporated in concrete for the construction of pavements. It is ideal for low-volume rural roads as well as urban pavements, adhering to the standard guidelines to fulfill the requirement of flexural strength of concrete.

Acknowledgment

The authors thank Malaviya National Institute of Technology, Jaipur, for supporting the research.

References

1 Kannur B & Chore H S, *Constr Build Mater*, 365 (2023) 130036.
2 Rakhimova G, *Int J GEOMATE*, 25 (110) (2023) 243.
3 Khichad J S, Vishwakarma R J &Bahekar P V, *Lect Notes Civ Eng*, 52 (2024) 281.
4 Khichad J S & Vishwakarma R J, *Int J Pavement Res Technol*, (2024) 1.
5 Alanazi H, Yang M, Zhang D & Gao Z, *Cem Concr Compos*, 65 (2016) 75.
6 Azarhomayun F, Haji M, Kioumarsi M & Shekarchi M, *Cem Concr Compos*, 125 (2022) 104276.
7 Herisson J, Guéguen-Minerbe M, van Hullebusch E D & Chaussadent T, *Mater Struct*, 50 (2017) 1.
8 Benhelal E, Zahedi G, Shamsaei E & Bahadori A, *J Clean Prod*, 51 (2013) 142.
9 Nguyen L, Moseson A J, Farnam Y &Spatari S, *J Clean Prod*, 185 (2018) 628.
10 Andrew R M, *Earth Syst Sci Data*, 10 (2018) 195.
11 Rojo-López G, Nunes S, González-Fonteboa B & Martínez-Abella F, *J Clean Prod*, 266 (2020) 121666.
12 Liu K, Shui Z, Sun T, Ling G, Li X & Cheng S, *Constr Build Mater*, 211 (2019) 120.
13 Reghunathan A K, Nazeer M & Kumar R A, *Int J Eng Adv Technol*, 3 (6) (2014) 176.
14 Liu Q, Qian Y, Li P, Zhang S, Wang Z, Liu J, Sun X, Fulham M, Feng D, Chen Z, Song S, Lu W & Huang G, *Acta Pharm Sin B*, 8 (3) (2018) 371.
15 Garas V Y & Kurtis K E, *Mag Concr Res*, 60 (7) (2015) 499.
16 Madandoust R & Mousavi S Y, *Constr Build Mater*, 35 (2012) 752.
17 Rashad A M, *Constr Build Mater*, 41 (2013) 303.
18 Avet F, Li X & Scrivener K, *Cem Concr Res*, 106 (2018) 40.
19 Asghari Y, EsmaeilMohammadyan-Yasouj S & Saeid Rahimian Koloor S, *Constr Build Mater*, 389 (2023) 131605.
20 Siddique R & Klaus J, *Appl Clay Sci*, 43 (3-4) (2009) 392.
21 Aashto: Standard Specifications for Transportation Materials and Methods of Sampling and Testing, 33rd Edition and AASHTO Provisional Standards, 2013 Khan M I & Siddique R, Resour Conserv Recycl, 57 (2011) 30.
22 Khan M I & Siddique R, *Resour Conserv Recycl*, 57 (2011) 30.
23 Shaikh F U A, *Constr Build Mater*, 43 (2013) 37.
24 Tassew S T & Lubell A S, *Constr Build Mater*, 51 (2014) 215.
25 Pakravan H R &Ozbakkaloglu T, *Constr Build Mater*, 207 (2019) 491.
26 Kizilkanat A B, Kabay N, Akyüncü V, Chowdhury S & Akça A H, *Constr Build Mater*, 100 (2015) 218.
27 Yin S, Tuladhar R, Shi F, Combe M, Collister T & Sivakugan N, *Constr Build Mater*, 93 (2015) 180.
28 Latifi M R, Biricik Ö & Mardani-Aghabaglou A, *J Adhes Sci Technol*, 36 (4) (2022) 345.
29 Aly T, Sanjayan J G & Collins F, *Mater Struct*, 41 (2008) 1741.
30 Banthia N & Gupta R, *Cem Concr Res*, 36 (7) (2006) 1263.
31 Leong G W, Mo K H, Loh Z P & Ibrahim Z, *Constr Build Mater*, 246 (2020) 118410.
32 Guerrero H, Alcocer S M, Carrillo J, Escobar J A & Hernandez H, *Eng Struct*, 275 (2023) 115281.
33 Alhozaimy A M, Soroushian P & Mirza F, *Cem Concr Compos*, 18 (2) (1996) 85.
34 Ali B, Qureshi L A & Khan S U, *Constr Build Mater*, 262 (2020) 120820.
35 Li Z, Shen A, Zeng G, Chen Z & Guo Y, *Mater Today Commun*, 33 (2022) 104824.
36 Kizilkanat A B, Kabay N, Akyüncü V, Chowdhury S & Akça A H, *Constr Build Mater*, 100 (2015) 218.
37 Singh A, Charak A, Biligiri K P & Pandurangan V, *Resour Conserv Recycl*, 182 (2022) 106304.
38 Chen Y, Cen G & Cui Y, *Constr Build Mater*, 192 (2018) 818.

39 Affan M & Ali M, *Constr Build Mater*, 323 (2022) 126599.
40 Ahmad J, Burduhos-Nergis D D, Arbili M M, Alogla S M, Majdi A & Deifalla A F, *Buildings*, 12 (11) (2022) 1951.
41 Liang N, You X, Yan R, Miao Q & Liu X, *Int J Concr Struct Mater*, 16 (1) (2022) 1.
42 Sun Z & Xu Q, *Mater Sci Eng A*, 527 (1-2) (2009) 198.
43 United Nations Development Programme, Sustainable Development Goals.
44 Bureau of Indian Standards: IS 8112:1989: Specification for 43 grade ordinary Portland cement. (1989).
45 Sain A, Gaur A, Somani P, Khichad J S &Balotiya G, *Arab J Sci Eng*, (2024) 1.
46 Khichad J S, Vishwakarma R J, Morkhade S G & Mehndiratta S, *Struct Eng Mech*, 90 (2024) 177.
47 Singh H & Siddique R, *Constr Build Mater*, 348 (2022) 128659.
48 Indian Standards: Specification for Coarse and Fine Aggregates from Natural Sources For Concrete. IS. 383, (1970).
49 Mazloom M, Ramezanianpour A A& Brooks J J, *Cem Concr Compos*, 26 (4) (2004) 347.
50 Chen X, Zhou M, Shen W, Zhu G & Ge X, *Constr Build Mater*, 190 (2018) 680.
51 Akarken G & Cengiz U, *Appl Clay Sci*, 232 (2023) 106786.
52 Zibara H, Hooton R D, Thomas M D A & Stanish K, *Cem Concr Res*, 38 (3) (2008) 422.
53 Ul Haq I, Elahi A, Nawaz A, Qadeer Shah S A & Ali K, *Constr Build Mate*r, 345 (2022) 128223.
54 Harikaran M, Gokulakannan S, Loganathan A, Chandiran R D, Ajith M & Dhanasekar V, *Mater Today Proc*, (2023) in-press.
55 IS 7320: Specification for concrete slump test apparatus. (1974).
56 Tahwia A M, Mokhles M &Elemam W E, *Innov Infrastruct Solut*, 8 (2023) 1.
57 Indian Standard: IS 516 (Part-1 Sec-I). (2021).
58 Tantri A, Nayak G, Shenoy A, Shetty K K, Achar J & Kamath M, *Innov Infrastruct Solut*, 7 (5) (2022) 1.
59 Taguchi G, Introduction to Quality Engineering, (1986).
60 Vignesh R & Rahim A A, *Arab J Sci Eng*, 49 (4) (2024) 5027.
61 Huang M L, Hung Y H & Yang Z S, *Measurement*, 94 (2016) 284.
62 Das P P& Chakraborty S, *Int J Interact Des Manuf*, 17 (3) (2023) 1021.
63 Şimşek B, Ultav G, Korucu H &Yartaşi A, *Period Politech Chem Eng*, 62 (2018) 323.
64 Korucu H, Şimşek B &Yartaşı A, *Arab J Sci Eng*, 43 (2018) 6033.
65 Mitra A C, Jawarkar M, Soni T & Kiranchand G R, *Procedia Eng*, 144 (2016) 77.
66 Şimşek B, İç Y T & Şimşek E H, *Arab J Sci Eng*, 41 (2016) 1435.
67 Cihan M T & Avşar Y E, *Arab J Sci Eng*, 48 (4) (2023) 4439.
68 Indian Road Congress: Guidelines for Cement Concrete Mix Design for Pavements Indian Roads Congress (IRC: 44-2017).
69 Kannur B & Chore H S, *Eur J Environ Civ Eng*, 27 (2023) 3507.
70 Khichad J S, Vishwakarma R J & Ingle R K, *Indian Concrete J*, 96 (7) (2022) 35.
71 Khichad J S, Vishwakarma R J & Magade S B, *Mater Today Proc*, 77 (2023) 764.